Epithermal effects in muon-catalyzed *dt* fusion: Comparison of experimental data with theoretical calculations

M. Jeitler, W.H. Breunlich, M. Cargnelli, P. Kammel, J. Marton, N. Nägele, P. Pawlek, A. Scrinzi, J. Werner, and J. Zmeskal
Institut für Mittelenergiephysik, Austrian Academy of Sciences, A-1090 Wien, Austria

H. Bossy, H. Daniel, F.J. Hartmann, G. Schmidt, and T. von Egidy
Physik Department, Technical University of Munich, D-85747 Garching, Germany

C. Petitjean
Paul Scherrer Institute, CH-5232 Villigen, Switzerland

J. Bistirlich, K.M. Crowe, M. Justice, and J. Kurck
University of California and Lawrence Berkeley Laboratory, Berkeley, California 94720

R.H. Sherman
Los Alamos National Laboratory, Los Alamos, New Mexico 87545

W. Neumann
Eidgenössische Technische Hochschule, CH-8049 Zürich, Switzerland

M.P. Faifman
RRC Kurchatov Institute, Moscow 123182, Russia
(Received 17 August 1994)

Epithermal effects in muonic molecular formation were observed during experiments in a low-density deuterium-tritium gas target carried out at the Paul Scherrer Institute. The high molecular formation rate of "epithermal" (not yet thermalized) muonic tritium atoms was reflected by a strong fast component in the fusion neutron time spectra followed by a smaller "steady-state" component where molecular formation occurs mostly from thermalized ("cold") $t\mu$ atoms. Further experimental evidence for high epithermal $dt\mu$ molecular formation rates has been derived from measurements in triple H-D-T mixtures. First, theoretical calculations predicted strong resonances at high $t\mu$ kinetic energies and showed qualitative agreement with the observed experimental data, but yielded molecular formation rates that differed substantially from the observed values. At present, refined calculations are being carried out which may improve the agreement with experiment. Further experiments are being planned to clarify open questions.

PACS number(s): 36.10.Dr

I. INTRODUCTION

Negative muons (μ^-) in hydrogen may form atoms and molecules in the same way as electrons do. However, due to the muon's higher mass, these objects are much smaller than their "normal" counterparts. In fact, the radius of a muonic molecular hydrogen ion (e.g., $dt\mu$) is so small that the nuclei may tunnel the Coulomb barrier with a high probability and fuse with a rate of $\approx 10^{12}$ s^{-1} [1, 2].

The time necessary for the formation of muonic molecular ions via electron emission (Auger transitions) is relatively long compared to the muon lifetime of 2.2 μs. However, in the case of deuterium-deuterium ($dd\mu$) or deuterium-tritium ($dt\mu$) muonic molecular formation there also exist resonant processes

$$d\mu + \mathrm{D}A_{\nu_i=0,K_i} \rightarrow [(dd\mu)_{J=1,v=1}aee]_{\nu_f,K_f}$$

$$A(=\mathrm{H},\ \mathrm{D},\ \text{or}\ \mathrm{T};\ a=p,\ d,\ \text{or}\ t) \quad (1)$$

and

$$t\mu + \mathrm{D}A_{\nu_i=0,K_i} \rightarrow [(dt\mu)_{J=1,v=1}aee]_{\nu_f,K_f}$$

$$A(=\mathrm{H},\ \mathrm{D},\ \text{or}\ \mathrm{T};\ a=p,\ d,\ \text{or}\ t) \quad (2)$$

in which the energy set free by the formation of the muonic molecular ion $dd\mu$ or $dt\mu$ in the very weakly bound (i.e, highly excited) state with rotational quantum number $J = 1$ and vibrational quantum number $v = 1$ goes into the vibrational (ν_f) and rotational (K_f) excitation of the "electronic" molecule. These processes allow one to reach molecular formation rates that are several orders of magnitude higher than the muon's decay rate ($\lambda_0 \approx 0.455 \times 10^6$ s^{-1}).

If in this process the excitation energies of the quantum states (ν_f, K_f) that correspond to the strongest resonances are higher than the energy set free by the formation of the molecular ion, the missing energy may be derived from the kinetic energies of the muonic atom and

the molecule with which it collides. In this case, the highest molecular formation rates will be observed either at high temperatures, where both molecules and muonic atoms have high kinetic energies, or in cold hydrogen isotope mixtures, but with muonic atoms that have not yet been thermalized ("hot" or "epithermal" muonic atoms).

In fact, while for process (1) the strongest resonance seems to correspond to a low kinetic energy of the reaction partners $d\mu$ and D_2, in the case of $dt\mu$ formation by process (2) there is strong evidence for the existence of high-temperature and epithermal effects.

(i) In experiments [3, 4] carried out at Paul Scherrer Institute [(PSI), Switzerland, formerly Schweizerisches Institut für Nuklearforschung (SIN)], in low-density gas targets a strong and quickly decaying time component was observed (Fig. 1). After an initial misinterpretation in terms of hyperfine effects in analogy to the $dd\mu$ case, Kammel [5] as well as Cohen and Leon [6] subsequently interpreted this component as being due to nonthermalized $t\mu$ atoms. Such components were then seen in high-density targets as well. However, thermalization times scale with density and at high densities these components decay so quickly that their analysis becomes difficult.

(ii) Data taken at several different temperatures at LAMPF show that the cycling rate rises with temperature and does not yet level off at 800 K, the maximum temperature measured [7].

(iii) From the location of the resonance energies, which have been calculated to a very high accuracy, theory [8] predicts extremely high resonant molecular formation rates at kinetic $t\mu$ energies of several hundred meV, which corresponds to temperatures of several thousand kelvin (Fig. 4).

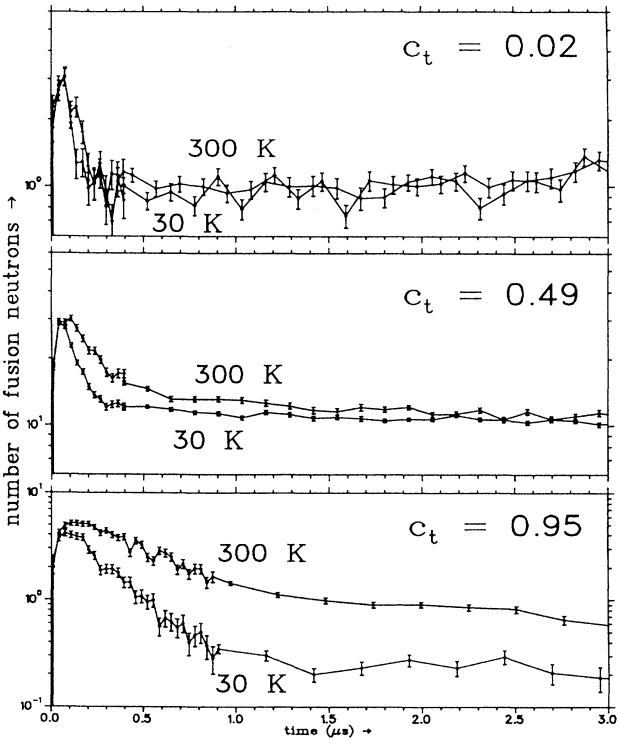

FIG. 1. Experimental time spectra of $dt\mu$ fusion neutrons measured in a deuterium-tritium target at $\Phi = 1\%$ of liquid hydrogen density.

It is highly desirable to understand the role of epithermal effects in muon-catalyzed fusion, not only to test the theory and to correctly interpret the contribution of nonthermalized $t\mu$ atoms to the steady-state cycling rate in hot or cold targets, but also to answer one of the fundamental questions in the context of a possible practical use of muon-catalyzed fusion: namely, which is the maximum cycling rate that can be attained?

One of the ways to obtain information about molecular formation rates at high kinetic energies would be to measure the fusion neutron flux from a target heated up to temperatures of several thousand kelvin. In spite of the obvious technical difficulties in working with tritium mixtures at conditions which can only be supported by very few materials, such measurements are currently being planned at PSI [9, 10].

Another ambitious experiment that would allow one to directly measure the epithermal molecular formation rates is being planned at TRIUMF (Canada). In this setup $t\mu$ atoms will evaporate from a thin layer of solid hydrogen and drift through vacuum to another thin layer of solid deuterium. The $t\mu$ kinetic energy will be determined by measuring the time of flight between these two layers. A similar experiment has already been carried out for $dd\mu$ fusion [11]. Working with tritium in such a setup, however, poses an additional experimental challenge.

The only approach that uses existing experimental data is to analyze the various components of the fusion neutron time distributions from the pioneering experiment in this field [3], where measurements were carried out in a low-density gas target at low and intermediate temperatures, and from subsequent experiments of our group that were done in H-D-T triple mixtures with high ^1H concentration [12]. In the present work these data have been analyzed in terms of molecular formation rates, scattering and transfer cross sections, and initial energy distributions of muonic atoms. Basic consistency with the theoretical picture has been found. However, several important discrepancies, especially with regard to molecular formation rates, have been established.

II. EXPERIMENTS

A. The D-T experiment

Measurements for this experiment were done at PSI in a deuterium-tritium gas target of low density at different tritium concentrations ($0.02 \leq c_t \leq 0.95$) and target temperatures ($30\ \text{K} < T < 300\ \text{K}$). Muons from the PSI accelerator muon beam with a momentum of 48.8 MeV/c entered the target vessel, which was set up in the PSI μE4 experimental area. Fusion neutrons from nuclear fusion following muonic molecular formation were measured by a neutron detector while muon and electron detectors served to define a time scale and to reduce background.

1. The target system

The target consisted of a cylindrical target cell (3 mm of copper with a 0.8-mm-thick silver window on either end) with a volume of about 1000 cm^3 filled with a gaseous deuterium-tritium mixture. The target cell and several muon and electron detectors were contained in a 5-mm steel vessel with a 0.25-mm steel entrance window (see Fig. 2). So, on their way into the target the muons had to pass through 0.25 mm of steel and 0.8 mm of silver. The 14.1-MeV neutrons from $dt\mu$ fusion that were to be observed had to pass through 3 mm of copper, 5 mm of steel, and about 10 mm of organic scintillation material (electron detectors) before they reached the neutron detector. The ^1H impurity was about 0.3% and could be neglected during the analysis. The gas pumping and storage system was situated inside a glovebox in the experimental area. Tritium and deuterium gas were passed through separate palladium filters before being mixed in the target cell. A total of 70 kCi of tritium (provided by the U.S. Department of Energy) was used in this experiment. A mass spectrometer was connected directly to the target cell and gas samples were taken before and after each run to determine the proportions of the different isotopic molecular populations. This was especially important because resonant molecular $dt\mu$ formation rates are supposed to depend strongly on the kind of molecule (D_2 or DT) encountered by the $t\mu$ atom. In other words, for a correct interpretation of the experiment it is not sufficient to merely know the atomic isotopic concentrations (which could be established by measuring the volume of deuterium and tritium gas filled separately into the target), but molecular concentrations must be known to a sufficient accuracy. If a statistical distribution of molecules is reached, the mixture is called "equilibrated":

$$c_{D_2} : c_{DT} : c_{T_2} = c_d^2 : 2c_d c_t : c_t^2 \ . \tag{3}$$

Complete equilibration may only be guaranteed at high temperature and after a sufficiently long period of time. Therefore, at low temperatures a measurement of molecular concentrations by mass spectrometry is indispensable. For a detailed description of the target filling procedure and mass spectrometry, see [10, 13].

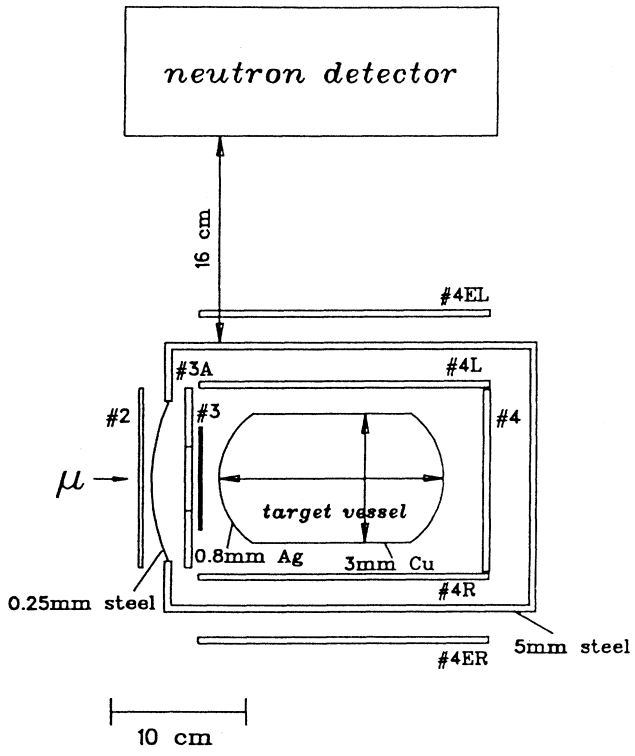

FIG. 2. Target and detector setup of the D-T experiment.

2. Detectors

(a) Neutron detector. The most important physical observable in this experiment was the time distribution of the 14.1-MeV fusion neutrons from the process

$$d + t \rightarrow \alpha + n \tag{4}$$

following $dt\mu$ molecular formation. The detector used for measuring these fusion neutrons was a NE213 (Nuclear Enterprises) liquid detector of rectangular shape ($28 \times 14 \times 10$ cm^3), which was equipped with two photomultipliers, one on each side. Liquid scintillation detectors of this kind allow one to discriminate between neutrons and γ quanta by pulse shape analysis [14, 15]. The detection of charged particles was avoided by demanding a prompt anticoincidence with a thin plastic scintillator positioned in front of the detector.

In a scintillation detector neutrons are detected via recoiling protons. Therefore, the measured energy is not the total energy of the neutron but an energy ranging between zero and the neutron energy, and incoming neutrons of one specific energy yield an energy distribution ("recoil spectrum") in the detector. It is not possible to use the whole spectrum because low-energy neutrons produced by other processes (muon-catalyzed *dd* or *tt* fusion, nuclear muon capture in the target cell) have to be suppressed by setting a sufficiently high energy threshold. With this threshold chosen at a neutron energy of 10 MeV, the neutron detector's total efficiency was $\sim 0.26\%$.

(b) Muon and electron detectors. The start signal for all measured time intervals was given by a telescope of muon counters in front of the target (the time between detection and muon stop in the target being negligibly short), while the stop signals were given by the neutron or electron detectors that had been hit by a particle. The muon telescope consisted of three scintillation counters (2, 3, and 3A). Counter 3A had a hole through which the muon had to pass to achieve a well collimated beam and to reduce the number of detected muons that stopped in the target cell wall. A muon stop signal was given by a coincidence of 2 and 3 in prompt anticoincidence with 3A and the electron detectors, which surrounded the target on all sides as far as possible. This allowed us to reject events where the muon passed through the target and left it through one of the electron detectors.

By this procedure it was possible to obtain a gas stop fraction of 9% at a gas density of 1% of liquid hydrogen

density, i.e., out of all events accepted as valid muon stops by the electronics, the muon stopped in the target gas in 9% of all cases, while in 91% it either stopped in the target cell wall or left the target undetected. Considering the low gas density this was a very satisfactory result. For one measurement made at a density of 0.5%, the gas stop fraction was 5%.

In order to avoid an overlay of fusion neutron time distributions from two different muons, events with two muons entering the target within less than 8 μs from one another were rejected as pileup. Rejection of capture neutrons from muons that stopped in the target wall was achieved by demanding detection of the muon's decay electron after the neutron. The total efficiency of the electron scintillation counters was 75%.

3. *Data analysis*

For data analysis clean time spectra of 14.1-MeV dt fusion neutrons were needed. A liquid scintillation detector of the type used records not only neutrons, but also other kinds of particles such as electrons from muon decay, γ quanta from electron bremsstrahlung, etc. Charged particles were suppressed by demanding an anticoincidence with the signal from an electron detector positioned between the target and the neutron detector. The probability of recording for γ's and electrons was strongly reduced by pulse shape discrimination.

The remaining background is neutrons from processes other than $dt\mu$ fusion: $dd\mu$ fusion, $tt\mu$ fusion, and muon capture in the target wall. Neutrons from $dd\mu$ and $tt\mu$ fusion have lower energies than $dt\mu$ fusion neutrons and were suppressed by setting a high-energy threshold (10 MeV). What remains is the high-energy tail of the neutrons produced by muon capture in the target walls. Due to the low gas-stop ratio of 9%, this background is very significant. However, it can be suppressed in an off-line analysis by demanding detection of the muon's decay electron in a certain time window after the neutron. Such a "delayed-electron" spectrum can contain neutrons from muon capture only if they were followed by an accidental electron. It will consist of the following types of events: (a) dt fusion neutrons followed by a muon decay electron, (b) accidental neutrons followed by a muon decay electron, (c) dt fusion neutrons followed by an accidental electron, (d) capture neutrons followed by an accidental electron, and (e) accidental neutrons followed by an accidental electron. When the raw neutron time spectrum is weighted by the measured mean number of accidental electrons in the time window (yielding c+d+e) and subtracted from the delayed-electron spectrum, only components (a) and (b) should remain. Component (b) can be calculated from the measured number of accidental neutrons and the measured electron time distribution and its subtraction should yield a clean spectrum of dt fusion neutrons followed by muon decay electrons. For a detailed discussion of this method, see [15–17].

A direct check of this method can be made by analyzing the spectra from a target filling that does not yield dt fusion neutrons. In this case the procedure described above should, within statistical errors, yield an empty spectrum. This test has been made and has shown that the spectrum still contains a certain number of events. It seems that there are slow secondary processes that give rise to an event in the electron detectors more than half a microsecond (the beginning of the time window for detection of the electron) after a neutron. The evaluation of the test allowed us to calculate the error in the neutron time distribution after the described background subtraction.

Due to the finite electron detection efficiency and the finite length of the time window for detection of the electron, a certain number of dt fusion neutrons ("good" events) is lost when this method is applied. As the neutrons from muon capture in the target cell materials disappear quickly—the muon lifetime in these materials is shorter by an order of magnitude than the free muon's lifetime — they need not be considered for the later part of the time spectrum ($t \gtrsim 1$ μs) so that one does not lose good fusion neutrons in this region where statistics is low due to muon decay.

Figure 1 shows experimental $dt\mu$ fusion neutron time spectra which were processed in the way described above, multiplied by $e^{\lambda_0 t}$ (λ_0 being the decay rate of the free muon) and normalized to the same number of muons. After 0.3–1.5 μs the spectra become flat, which means that in this region the fusion output is proportional to the number of muons and decreases with muon decay. There is an obvious strong dependence on the tritium concentration. The total fusion yield is highest at intermediate tritium concentrations and lower at both very low and very high c_t where deuterium-tritium transfer or molecular formation, respectively, become slow. The initial peak due to molecular formation by epithermal $t\mu$ atoms gets wider as the tritium concentration rises, which is explained by the low scattering cross sections for $t\mu$ atoms on tritons.

The temperature dependence strongly varies with the tritium concentration. While at low tritium concentrations ($c_t \leq 0.1$) spectra taken at 30 K and at 300 K show no difference within errors, at higher tritium concentrations the fusion yield at room temperature is substantially larger than at cryogenic temperatures.

In the investigated region of target densities (0.5–1 % of liquid hydrogen density), all scattering and molecular formation rates show a purely linear density dependence as opposed to high-density targets (cf. [18–20]). While the initial peak in the time spectra has to be described by a more or less complex kinetical model the later, flat part of the spectra allows us to use the simple phenomenological concept of the cycling rate λ_c, which is defined as the inverse of the mean time between two subsequent dt fusions catalyzed by the same muon and is usually normalized to liquid hydrogen density (4.25×10^{22} atoms/cm^3). The values in Table I and in Fig. 3 were obtained by a fit over the time range from 1.5 to 6 μs for $c_t \leq 0.5$ and from 3 to 6 μs for higher tritium concentrations. The statistical errors can be seen from Fig. 3. The total error is in all cases dominated by the 10% overall error in the neutron detection efficiency. The data agree well with other measurements taken at similar conditions [19, 21].

TABLE I. Steady-state cycling rates (μs^{-1}) for various combinations of target temperatures and relative tritium concentrations.

c_t	30 K	100 K	200 K	300 K
0.02	3.6			4.0
0.10	24	23		22
0.23				49
0.42				55
0.49	39	43	44	48
0.88	3.9	3.9	4.4	7.4
0.95	0.74			2.2

B. The H-D-T experiment

An experiment with a gas target consisting of a mixture of all three hydrogen isotopes H, D, and T was carried out at PSI. The most abundant isotope was ^{1}H with its concentration c_p ranging from 0.90 to 0.97, followed by deuterium with c_d between 0.10 and 0.03. The tritium concentration was extremely low and ranged between 0.36×10^{-3} and 0.47×10^{-3}. The primary aim of this experiment was to directly measure the sticking coefficient ω_s in $dt\mu$ fusion, which is the probability that after a muon-catalyzed dt fusion the muon is not set free ($t\mu + d \rightarrow dt\mu \rightarrow \alpha + n + \mu$), but remains bound to the ^{4}He nucleus ($t\mu + d \rightarrow dt\mu \rightarrow \alpha\mu + n$). The experimental setup and the evaluation of the sticking coefficient have been described in detail elsewhere [12].

The main detector was the target cell itself, which was structured as a high-pressure ionization chamber. Due to the different electric charge of the reaction products α^{2+} and $(\alpha\mu)^+$, their tracks in the ionization chamber are of different length, which influences the recombination process of the formed ion-electron pairs and thus results in different energy signals in the ionization chamber for α^{2+} and $(\alpha\mu)^+$. The extremely low tritium concentration had to be chosen to reduce background in the ionization chamber's signal due to noise from tritium β decay. Due to the high ^{1}H concentration, muons are mostly captured by protons to form $p\mu$ atoms after which they are transferred with very high rates [29] to deuterons or tritons to form $d\mu$ or $t\mu$ atoms.

While the ionization chamber makes it possible to directly differentiate α^{2+} and $(\alpha\mu)^+$ events, its time resolution of several hundred nanoseconds does not allow one to get detailed information on the time structure. So an array of 20 neutron detectors surrounding the active target cell was used to detect the fusion neutrons and record their time spectra. The array consisted mostly of plastic scintillation detectors, which do not offer the possibility to suppress background from bremsstrahlung γ's by pulse shape discrimination, but by using the ionization chamber as a trigger detector selecting only fusion events sufficiently clean neutron time spectra could be obtained.

Although the target density was much higher than in the case of the D-T experiment (17% instead of 1% of liquid hydrogen density), the high ^{1}H concentration and the fact that $d\mu$ and $t\mu$ scattering cross sections on protons are very small (due to a Ramsauer-Townsend effect) created a time scale for the $d\mu$ and $t\mu$ thermalization process similar to that in the D-T experiment. One may say that after the fast $p \rightarrow d$ or $p \rightarrow t$ muon transfer the protons become invisible and the further kinetics evolve as in a deuterium-tritium target of correspondingly lower density, with the one important exception that most deuterons (with which molecular formation and subsequent fusion may occur) are bound not in D_2 or DT molecules, but in HD molecules.

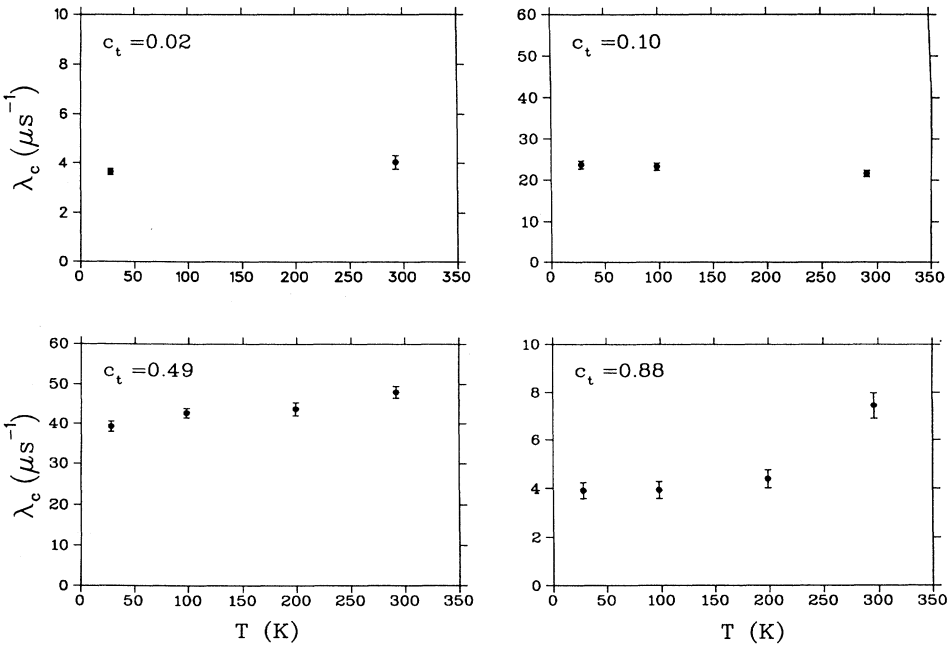

FIG. 3. Temperature dependence of normalized cycling rates in a deuterium-tritium target at four different tritium concentrations.

III. ANALYSIS

A. Basic processes

In order to compare experimental neutron time distributions with theoretical predictions, the competing processes of thermalization (slowing down) of $t\mu$ atoms and epithermal molecular formation must be considered and theoretical fusion neutron time distributions must be calculated by including the following parameters: (i) the $dt\mu$ molecular formation rates of reaction (2) dependent on the center-of-mass kinetic energy of the $t\mu$–DA (A=D, T, or H) system, the kind of molecule (D_2, DT, or HD) that forms a compound molecule with the $t\mu$ atom, the initial rotational state K_i of the molecule (depending on the target temperature), and the hyperfine spin state of the $t\mu$ atom ($F = 0$ or $F = 1$); (ii) the differential scattering cross sections of $t\mu$ and $d\mu$, dependent on the center-of-mass kinetic energy of the collision partners, the collision partner (d or t nuclei bound in molecules D_2, DT, or T_2), the scattering angle, the final spin state of the $t\mu$ atom (conservation of spin or spin flip by charge exchange on a t nucleus), and the change of the total energy available in the center-of-mass system due to spin flip or because of rotational or vibrational excitation of the colliding molecule (depending on its initial rotational state K_i and thus on the target temperature); (iii) the energy-dependent rate of the transfer process $d\mu + t \rightarrow t\mu + d$ in the ground state and in excited states; and (iv) the initial kinetic energy distribution of $t\mu$ and $d\mu$ atoms.

1. *Molecular formation rates*

Resonant and nonresonant $dt\mu$ molecular formation rates for process (2) as functions of $t\mu$ kinetic energies in cold targets of various temperatures have been calculated by Faifman and co-workers [8]. These calculations have yielded very high rates of up to 10^{10} s^{-1} at $t\mu$ kinetic energies of several hundred meV (cf. Fig. 4). The different peaks in the figures correspond to different vibrational transitions to the excited final state of the mesic molecular complex, whereas the individual rotational transitions cannot be resolved due to averaging over the thermal motion of the target molecules. While at room temperature or below molecular $dt\mu$ formation by thermalized $t\mu$ atoms nearly always results in nuclear fusion, at high $t\mu$ kinetic energies backdecay may be significant (according to [8] up to 45%) and must be included in a calculation of the muon-catalyzed fusion kinetics.

2. *Scattering rates*

The fusion neutron output is mainly determined by the competition between molecular formation, on the one hand, and the slowing down of $t\mu$ atoms by scattering processes, on the other hand. So, in order to calculate the neutron time distributions from theory one needs not only the molecular formation rates, but also the rates for scattering on the target molecules. What is important is

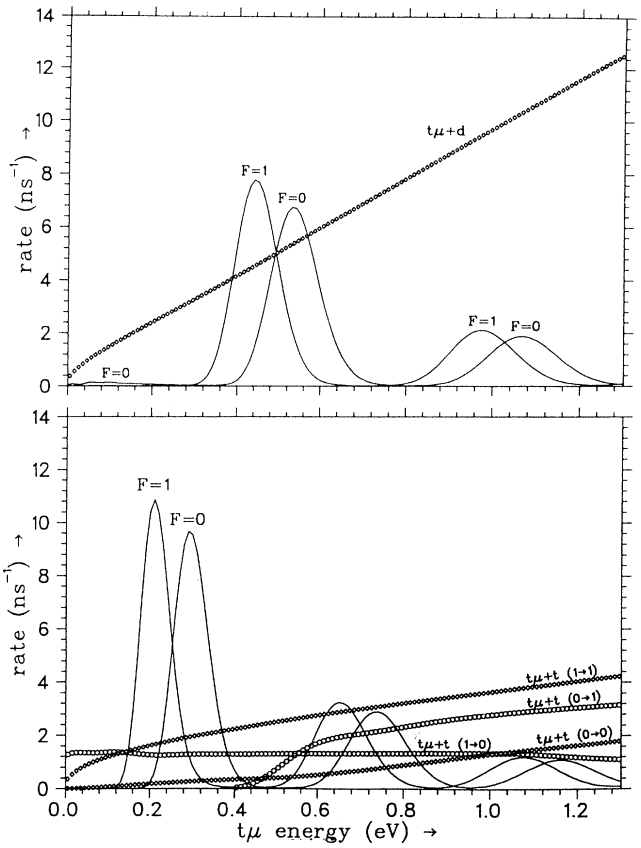

FIG. 4. Rates of processes to which $t\mu$ atoms are subject in a deuterium-tritium target. The top frame shows the processes that are important at low tritium concentrations (elastic scattering on deuterons and molecular formation on D_2 molecules). The bottom frame shows processes that become increasingly important as the tritium concentration rises (elastic and spin-flip scattering of $t\mu$ atoms in both hyperfine states on tritons and molecular formation on DT molecules).

not the number of scattering processes, but the energy loss. The energy (in the laboratory system) of the outgoing particle depends upon the scattering angle. Therefore it is not sufficient to know the total cross sections σ, but differential cross sections $d\sigma/d\Omega$ are needed.

Various calculations of the cross sections for the scattering of muonic hydrogen isotope atoms on hydrogen isotope nuclei have been carried out by using different methods [22–24]. The results are in satisfactory agreement. The present analysis is based on [23]. For the scattering of muonic tritium the cross sections show a strong dependence on the collision partner (proton, deuteron, or triton), the collision energy, and, for scattering on tritons, on the $t\mu$ hyperfine state. By far the largest elastic scattering cross sections have been calculated for $t\mu + d$ scattering. This dominant process shows a strong p-wave contribution, which is due to the existence of the weakly bound state $(dt\mu)_{J=1,v=1}$, the very state that makes resonant $dt\mu$ molecular formation possible. This contribution results in an important angular anisotropy: $t\mu + d$ scat-

tering is strongly forward peaked and the mean energy loss per collision is smaller than in other elastic scattering processes (Fig. 5).

In reality muonic atoms collide not with nuclei, but with molecules. So, for an exact calculation, effects resulting from scattering on the electron shell ("electron screening") and from the molecular structure of the target particle (two nuclei bound together) should be considered. Calculations that include both effects [25] or only the effect of electron screening [24] have yielded significantly higher total cross sections for low collision energies. However, the additional scattering contribution is strongly forward peaked [26] and therefore not of great importance for the thermalization process.

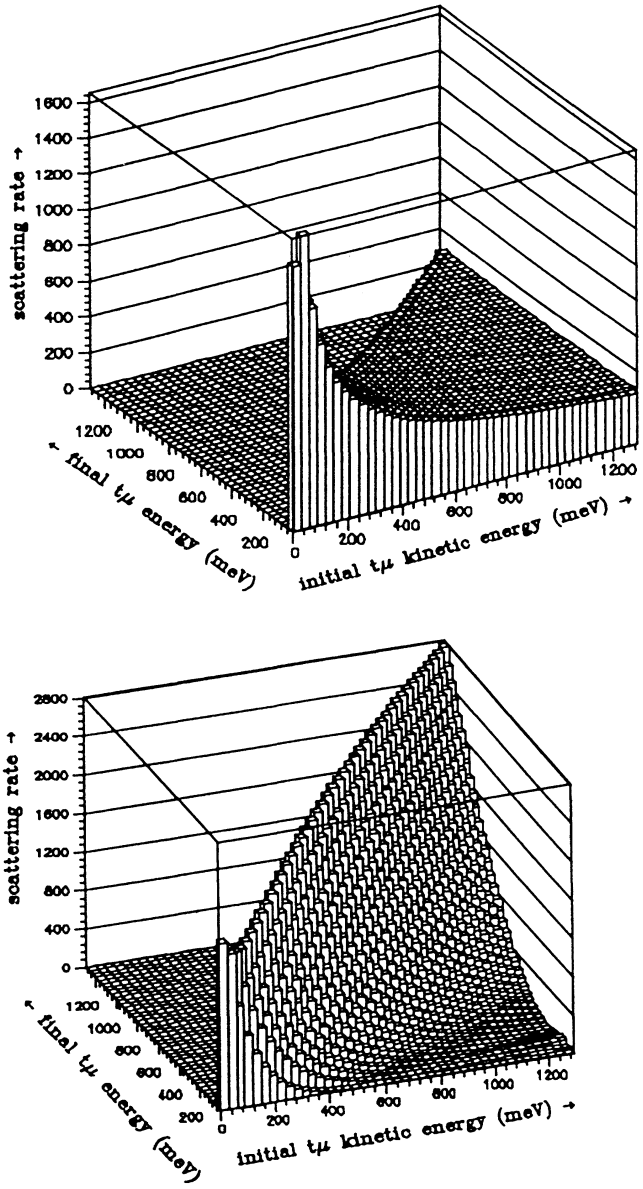

FIG. 5. $t\mu$ energy distribution before and after elastic scattering for isotropic ($t\mu_{F=1} + t \rightarrow t\mu_{F=1} + t$, top) and for anisotropic ($t\mu + d$, bottom) scattering.

3. Deuterium-tritium transfer

Resonant $dt\mu$ molecular formation is possible only if the muon was originally bound to the triton. So, when at high deuterium concentrations the muon is first captured by a deuteron with high probability, resonant molecular formation must be preceded by deuterium-tritium transfer. This transfer may occur either before complete deexcitation of the $d\mu$ atom (with the main quantum number $n > 1$) or after its deexcitation, i.e., from the $1s$ state. In the following, q_{1s} will denote the probability that a $d\mu$ atom formed in a highly excited state reaches the $1s$ state (in other words, that no transfer occurs before complete deexcitation) and λ_{dt} will refer to the rate of deuterium-tritium transfer in the $1s$ state.

Atomic muon capture by a triton or deuteron occurs in an excited state with $n \geq 14$. Subsequently, the muonic hydrogen atom deexcites to the $1s$ state within less than $10^{-11}\ \Phi^{-1}$ s, Φ being the target density relative to liquid hydrogen. Theoretical calculations [27] have suggested the existence of a quasiresonant charge-exchange process $(d\mu)_n + t \rightarrow (t\mu)_n + d$ in quantum numbers $2 \leq n \leq 5$ that is fast enough to compete with the deexcitation rate. The resulting values for q_{1s} are significantly different from unity, i.e., a significant percentage of muons is expected to be transferred to the triton before the $(d\mu)_{1s}$ state is reached.

There are no direct experimental measurements of q_{1s} yet. Experiments (cf. [2]) contradict the strong dependence of q_{1s} on target density and tritium concentration predicted by [27] and suggest that q_{1s} is closer to unity than calculated. Recent experiments carried out at PSI [28] for H-D mixtures show that in the analogous case of $p \rightarrow d$ muon transfer, excited-state transfer is significant, but weaker than calculated.

For the ground-state transfer rate λ_{dt} there are numerous calculations and experimental measurements (for a survey see [2]). However, the interpretation of experimental results is not completely straightforward due to our incomplete knowledge of the $dt\mu$ reaction kinetics (in particular, the value of q_{1s} and hyperfine effects in $dt\mu$ molecular formation). Calculations indicate that the transfer rate depends on the collision energy of the $d\mu$ atom and the t nucleus and rises steeply at higher energies [29]. So, for an exact calculation of fusion neutron time distributions it is necessary to consider the competing processes of $d \rightarrow t$ transfer and $d\mu$ thermalization by elastic scattering. The present analysis has been based on calculations of λ_{dt} that include the effects of molecular structure [29] and on the $d\mu$ scattering rates published in [23].

4. The initial energy distribution of $t\mu$ and $d\mu$ atoms in the 1s state

In the case of $t\mu$ formation by muon transfer in the ground state from a $d\mu$ or $p\mu$ atom, the $t\mu$ atom is formed with a high initial kinetic energy (19 and 46 eV, respectively), which is well above the important molecular formation resonances predicted by theory. If a muonic hydrogen isotope atom is formed directly by muon capture,

this occurs in a highly excited state ($n \geq 14$). While the muonic cascade is very fast, scattering rates in excited states could be so high as to compete with deexcitation. On the other hand, calculations [30, 31] propose that $t\mu$ atoms thermalized during early stages of the cascade may be reaccelerated by processes such as $(t\mu)_n + T_2 \rightarrow (t\mu)_{n-1} + T_2{}^+ + e$. According to [31], at a density of $\Phi = 1\%$ of liquid hydrogen density, 40% of all thermalized $t\mu$ atoms are reaccelerated to an energy of ~ 0.5 eV.

There are no direct experimental measurements of the initial energy distribution of $t\mu$ atoms. Measurements for muonic deuterium carried out at PSI showed that the initial $d\mu$ distribution could be fitted by a Maxwellian whose effective temperature corresponds to 1.4 ± 0.2 eV [32].

B. Monte Carlo calculations

Due to the complexity of the theoretical input data (molecular formation rates, scattering cross sections, and transfer rates), all of which are energy dependent, a Monte Carlo code was developed for calculating the thermalization of muonic atoms and the theoretical neutron time distributions. This program follows the histories of individual muons, one at a time from time zero (the moment the muon enters the target) up to the maximum time of interest (several muon lifetimes). The kind of atom formed by the muon ($t\mu$, $d\mu$, or $p\mu$), its energy, and spin state are recorded and placed in histograms. The kind of interactions undergone by muonic atoms (isotopic transfer, elastic scattering, spin flip, and molecular formation) and molecules (fusion and backdecay), the energy of muonic atoms after the interaction and the time intervals between two interactions are chosen at random according to the probabilities calculated from the corresponding rates. For a detailed description of the program see [33].

As an example, Fig. 4 shows for a deuterium-tritium target of a temperature of 30 K the total interaction rates for $t\mu$ atoms that are significant at low tritium concentrations (top: elastic scattering on deuterons and molecular formation by collision with D_2 molecules) and the rates that become important at high tritium concentrations (bottom: elastic scattering and spin flip on tritons and molecular formation on DT molecules). The molecular formation rates have been taken from [8], while the other rates have been calculated from the cross sections published in [23].

1. *Energy spectra*

To illustrate the importance of epithermal molecular formation one can look at the overlap of the $t\mu$ energy distribution at a certain time with the resonances in the molecular formation rates. As the position and size of these resonances depend on the hyperfine state, it is necessary to do this for one definite hyperfine state. Figure 6 shows this comparison for the $F = 0$ state. The large population of energetic $t\mu$ atoms at the time shown (30 ns) illustrates the significance of epithermal molecular formation. The epithermal resonances in the molecular formation rates are so big that they strongly influence the energy distribution of muonic atoms. Near the strongest resonances the number of $t\mu$ atoms is diminished because they are being absorbed by molecular formation. It is important to correctly consider this effect of "burning out" (cf. also [34]). Calculating the $t\mu$ energy distribution by merely including scattering processes and then integrating it over the molecular formation rates would quite obviously yield a wrong result.

The thermalization of energetic $t\mu$ atoms in a deuterium-tritium mixture strongly depends on the relative isotopic concentrations (Fig. 7), due to the following reasons.

(i) At $t\mu$ energies $\lesssim 0.5$ eV ($\approx 2\Delta E^{\rm hfs} = 2 \times 0.237$ eV) and high tritium concentrations, the rate for process $t\mu_{F=1} \rightarrow t\mu_{F=0}$ is high, while the inverse process is strongly suppressed because of energy conservation. So after a certain time most muonic tritium atoms are in their lower hyperfine state and scattering on tritium is dominated by the elastic process $t\mu_{F=0} \rightarrow t\mu_{F=0}$. The total cross section for this process is smaller, by more than one order of magnitude, than the cross section for elastic scattering on deuterons.

(ii) For scattering on deuterons (which is the dominant process at high and intermediate deuterium concentrations due to the large total cross section) the p-wave contribution is very important so that the mean energy loss during one scattering process on a deuteron is less than during scattering on a triton. Thus, for $t\mu$ energies $\gtrsim 0.5$ eV the slowing-down process is more efficient at high c_t than at high c_d. Another effect visible in the spectrum is that due to the collision kinematics, the $t\mu$ atom cannot lose more than $1 - [(m_{t\mu} - m_d)/(m_{t\mu} + m_d)]^2$ or $\sim 96\%$ of its energy during one collision with a deuteron that is at rest.

(iii) As soon as a $t\mu$ atom has been formed, the probability for $dt\mu$ molecular formation rises with the deu-

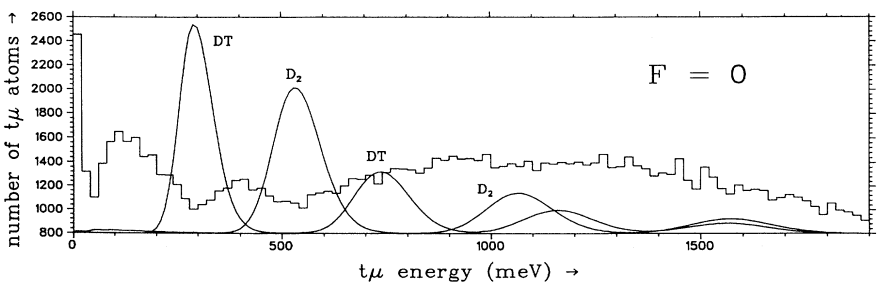

FIG. 6. Calculated $t\mu_{F=0}$ energy distribution at time $t =$ 30 ns (histogram) and epithermal molecular formation rates. The energy distribution gets "burned out" in the region of the strong resonances.

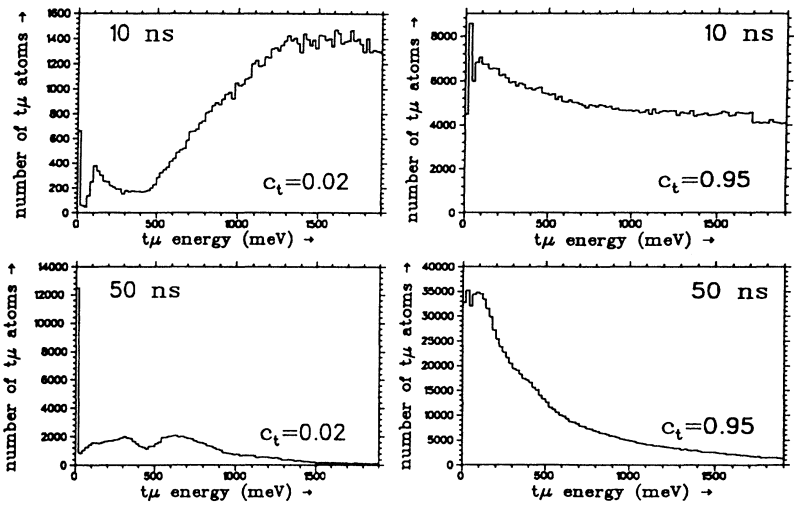

FIG. 7. Development in time of $t\mu$ energy distributions in a deuterium-tritium target at low and high c_t.

terium concentration. For epithermal molecular formation the backdecay probability is rather high (up to about 50% [8]). If one assumes that backdecay always produces thermalized $t\mu$ atoms, this leads to the quick development of a narrow peak of thermalized $t\mu$ atoms at high deuterium concentrations.

So far the thermalization of initially "hot" $t\mu$ atoms has been described. For $t\mu$ atoms formed not by transfer processes but by direct atomic muon capture, the real form of the initial $t\mu$ energy distribution is not known. What counts for molecular formation is not the exact energy of a $t\mu$ atom, but only whether its energy is above or below the major resonances. In the present calculations we therefore simply assumed a certain fraction $p_{\rm th}$ of the $t\mu$ atoms not formed by transfer to be thermalized from the beginning while the rest was supposed to have an initial energy of 2 eV, which is well above the calculated molecular formation resonances.

Figure 8 was calculated for $p_{\rm th}$=0.5. Apart from the large amount of thermalized atoms in the first bin there is a characteristic high peak at an energy of $\sim$ 0.12 eV caused by $t\mu_{F=0}$ atoms that were originally formed in the F=1 state with thermal energy and gained energy during spin flip by charge exchange ($t\mu_{F=1} + t \rightarrow t\mu_{F=0} + t +$ 0.237 eV). Due to the nearly equal masses of the $t\mu$ atom and the triton, each of them carries away about half of the hyperfine splitting energy.

The "steady state." At the given density of Φ=1% in a deuterium-tritium target the $t\mu$ energy spectrum changes most strongly during the first microsecond after the muon entered the target. At intermediate tritium concentrations ($0.2 < c_t < 0.8$) an equilibrium between the different states in which the muon may be found ($d\mu, t\mu_{F=1}, t\mu_{F=0}$, etc.) and stable energy distributions of muonic atoms are established. Due to the recycling of muons after fusions, the energy distributions differ significantly from a Maxwellian (Fig. 9, center).

At the same density but very low or very high tritium concentrations the steady state is approached far more slowly and practically never reached while the muon is still "alive." Even without any recycling (when setting the molecular formation rate in the Monte Carlo program equal to zero) the $t\mu$ energy spectrum after many muon lifetimes still differs from a Maxwellian. At low tritium concentrations (Fig. 9, left) this is due to the slow transfer process from deuterium to tritium (at c_t=0.01 the effective transfer rate would be $\Lambda_{dt} = \Phi c_t \lambda_{dt} \approx 0.01 \times 0.01 \times 3 \times 10^8\ {\rm s}^{-1} = 0.03\ \mu{\rm s}^{-1}$), which yields $t\mu$

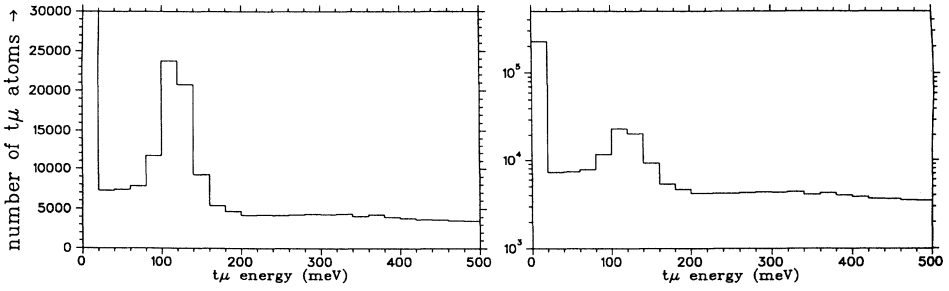

FIG. 8. $t\mu$ energy distribution after 50 ns in a deuterium-tritium target (c_t = 0.5) under the assumption that half of all $t\mu$ atoms formed by muon capture are initially thermalized ($p_{\rm th}$ = 0.5). The left-hand frame shows the energy distribution on a linear scale, with the first bin being cut off. The right-hand frame shows the same distribution on a logarithmic scale.

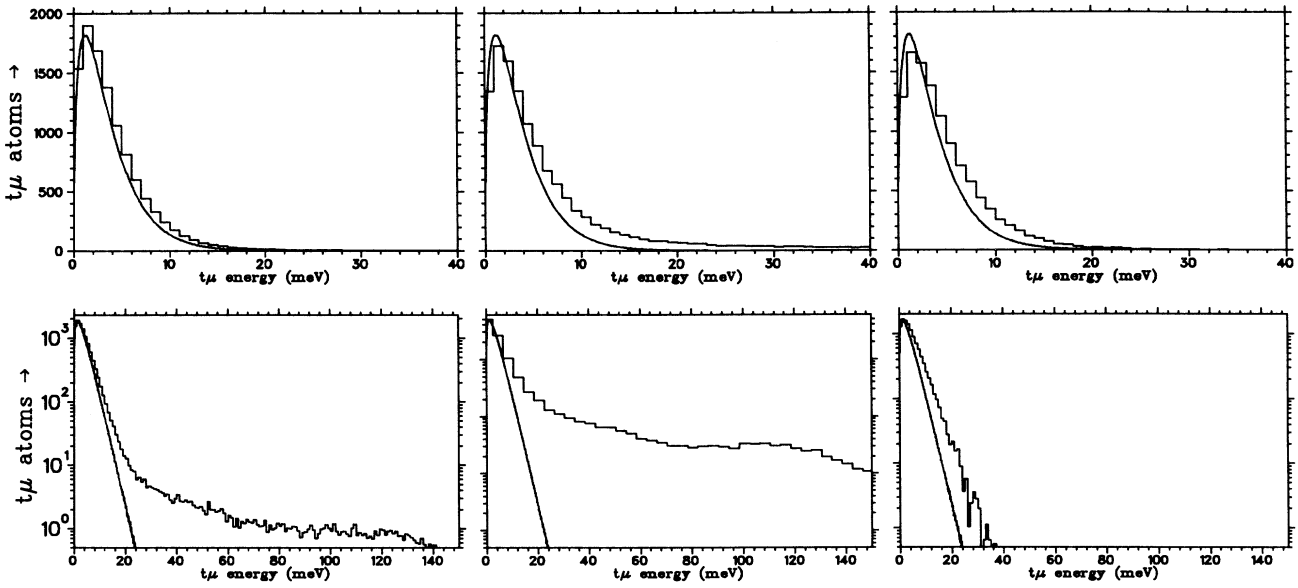

FIG. 9. Maxwell distributions for a temperature of 30 K and calculated $t\mu$ energy distributions after ten muon lifetimes at low, intermediate, and high tritium concentrations (top, linear; bottom, logarithmic scale).

atoms with an energy of 19 eV even after many microseconds. At high tritium concentrations (Fig. 9, right) the $F = 1$ state depopulates quickly and most $t\mu$ atoms soon reach energies below 0.1 eV in the $F = 0$ state. The further slowing down, however, is determined by the low elastic scattering rate for low-energy $t\mu$ atoms in this state ($\sim 0.045\ \mu s^{-1}$ at $E_{t\mu} = 0.01$ eV, $c_t \sim 1$, and $\Phi = 1\%$). This shows that at certain target conditions the relative abundance of the various states of the muon ($d\mu, t\mu_{F=1}, t\mu_{F=0}$, etc.) will not reach a constant value within the time accessible to experiment (a few muon lifetimes). Still, the term "steady state" will be used for the region of the time spectra where the observed fusion neutron output shows no changes except for the exponential decrease caused by muon decay.

So we have shown that at the density considered (Φ=1%), the $t\mu$ energy distribution in a deuterium-tritium mixture differs from a Maxwellian for all relative isotopic concentrations and it would be incorrect to calculate "effective rates" for a certain temperature by integrating energy-dependent rates of physical parameters over the corresponding Maxwell distribution. Most of what has been said also applies to processes in a mixture of all three hydrogen isotopes (H-D-T). Scattering on protons may be neglected because the cross section for $t\mu + p$ is far smaller than for $t\mu + d$ or $t\mu + t$. At very high ^{1}H concentrations most muons will originally form $p\mu$ atoms and quickly transfer to deuterons or tritons because of the very high transfer rates (cf. [29]), while direct formation of $d\mu$ or $t\mu$ atoms by atomic muon capture will be negligible. So our lack of information on the initial energy distribution of $t\mu$ atoms formed in this way will not affect the data analysis for such an experimental setup. All $d\mu$ or $t\mu$ atoms formed in this way will initially have the high kinetic energy gained during the transfer from $p\mu$ (about 45 eV), which is far above the initial energy of $d\mu$ or $t\mu$ atoms formed by direct muon capture. Epithermal molecular formation and epithermal $d \rightarrow t$ transfer will play a more important role than in a deuterium-tritium target.

2. *Fusion neutron spectra*

Apart from the $t\mu$ energy distribution discussed above, the Monte Carlo program histograms the fusion neutron output (i.e., molecular formations not followed by backdecay) for each time and each $t\mu$ energy. Figure 10 shows this histogram for a cold target ($T = 30$ K) consisting of equal amounts of tritium and deuterium ($c_t = c_d = 0.5$). Muon decay is not considered. The individual molecular formation resonances may be easily identified. At room temperature both energy distributions and molecular formation resonances are smeared out and it is not so easy to separate the contributions from the various resonances.

At very low energies (Fig. 10, left) there are fusion events from thermalized $t\mu$ atoms. The corresponding molecular formation rates are small (at 30 K the dominant rate $\lambda_{dt\mu-d}^{F=0} \sim 10^8\ s^{-1}$ normalized to liquid hydrogen density), but the muonic atoms remain in this state until molecular formation occurs. Therefore, as soon as a sufficient number of $t\mu$ atoms has been thermalized (low-energy buildup at early times in the spectrum) fusion output from this region is significant. At high energies the epithermal molecular formation resonances appear. They are most prominent at the beginning of the time

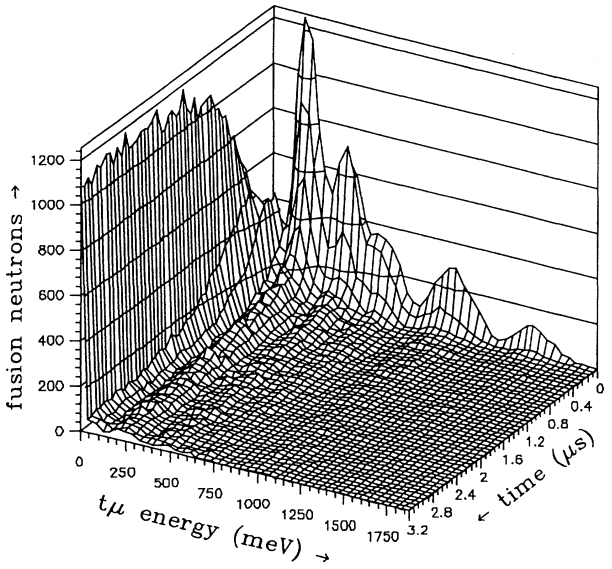

FIG. 10. Number of $dt\mu$ fusion neutrons for time t after entry of the muon into the target and the kinetic energy of the $t\mu$ atom that produced the fusion. Target conditions: T = 30 K, $\Phi = 1\%$, $c_t = 0.5$, and $p_{\rm th} = 0.5$.

axis because of the large number of epithermal $t\mu$ atoms at early times.

Due to muon recycling after fusions, the epithermal contribution does not die out completely even after a few microseconds when all originally formed muonic atoms should have been thermalized. This shows that even in the steady state (which is quickly reached at high target densities), epithermal molecular formation has to be considered for a correct analysis. The fraction η of dt fusions in the steady state that are due to nonthermalized $t\mu$ atoms strongly depends on the relative isotopic concentrations. At high deuterium concentration c_d the muonic tritium will most often collide with a deuteron and thus has a fair chance of forming a $dt\mu$ molecular ion while still "hot," whereas at low c_d it will first lose energy in collisions with other nuclei. This explains why, in spite of higher $t\mu + d$ scattering cross sections and consequently faster $t\mu$ thermalization at high c_d, the value of η calculated by the Monte Carlo program drops from ~0.4 in a target consisting mostly of deuterium ($c_t < 10\%$) to less than 0.1 at $c_t > 0.9$.

C. Comparison of theoretical and experimental fusion neutron time distributions in a deuterium-tritium target

The main aim of the Monte Carlo simulation was to calculate fusion neutron time spectra and then compare them with the experimental spectra. All information about the kinetic energy and the hyperfine state of $t\mu$ atoms, thermalization by scattering or backdecay, spin-flip processes, etc., is useful to obtain a clearer picture of the $dt\mu$ kinetics, but cannot be directly checked by the data from our experiments.

Figure 11 shows a comparison of experimental neutron time spectra for various tritium concentrations and two different target temperatures with the Monte Carlo spectra. The molecular formation rates were taken from [8]. Half of all $t\mu$ atoms formed by direct atomic muon capture (not by transfer) were supposed to be thermalized from the beginning ($p_{\rm th} = 0.5$ [31]). Ground-state $d \rightarrow t$ transfer rates were taken from [29]. For excited-state transfer, values for q_{1s} obtained from [21] were used (see Table II).

Although the overall structure of the experimental spectra is reproduced, it is obvious that there are major discrepancies. For a target temperature of 30 K, (i) the theoretical fusion neutron output in the steady state is too low (especially at intermediate tritium concentrations c_t); (ii) at intermediate c_t the theoretical spectra show a slow decrease and the steady state is reached much later than in the experimental spectra; (iii) at low c_t the theoretical spectra show a buildup which is practically invisible in the experimental spectra; and (iv) the epithermal peak in the Monte Carlo spectrum for $c_t = 0.95$ is somewhat higher than in the experimental spectrum.

At 300 K it is obvious that the calculated fusion neutron output is far too high. The calculations for temperatures of 100 K and 200 K also overestimate the fusion yield, although the discrepancy there is somewhat smaller.

Before looking for possible errors in the theory, the maximum possible deviations due to errors in the experimental parameters have to be considered.

(i) The overall error in the neutron detection efficiency is about 10%. However, this error affects all spectra in the same way, i.e., the neutron time spectra for all tritium concentrations and target temperatures measured might have to be scaled up or down by up to 10%, but their shape and relative size are not affected by this error.

(ii) The atomic concentrations c_t and c_d and the molecular concentrations $c_{\rm D_2}$, $c_{\rm DT}$, and $c_{\rm T_2}$ (i.e., the degree of equilibration of the target) as well as the target density Φ are known to an accuracy of about 10%. A variation of the target parameters within the calculated errors results in a change of the fusion yield of less than 5% at low and intermediate tritium concentrations ($c_t \leq 0.5$) and of about 10% at high tritium concentrations (this is due to the somewhat higher relative error in the D_2 concentration at high c_t). Obviously the resulting change

TABLE II. Excited-state transfer.

c_t	q_{1s}
0.02	0.97
0.10	0.87
0.49	0.57
0.88	0.41
0.95	0.40

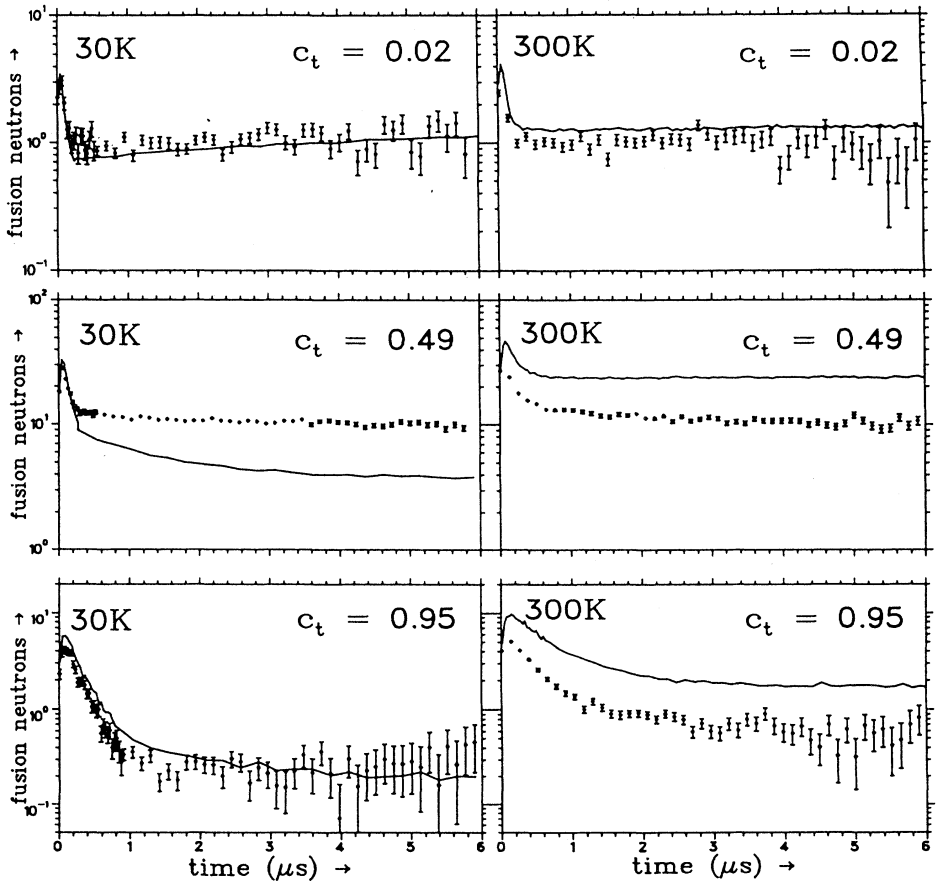

FIG. 11. Comparison of experimental (error bars) and calculated fusion neutron time distributions (see text for parameters used).

cannot account for the discrepancy between the Monte Carlo and the experimental spectra.

(iii) The variation in the target temperature was less than 2% and its effect on the calculated molecular formation rates is negligible.

(iv) The background caused by neutrons from nuclear muon capture and by accidentals that remains after applying the background subtraction procedure described above is only a few percent in the worst cases (in the early time region of spectra with low fusion-yield conditions) and below 1% otherwise.

The following theoretical parameters may be modified to achieve a better fit of the data: molecular formation rates, scattering rates, the transfer rate λ_{dt} and the parameter q_{1s} describing transfer in excited states, and the initial energy distribution of $t\mu$ atoms formed by muon capture.

1. *Molecular formation rates*

To find out how molecular formation rates should be modified to better reproduce the experimental spectra it is useful to split up the Monte Carlo spectra into four components corresponding to the four possible molecular formation processes (a $t\mu$ atom with $F = 0$ or $F = 1$ colliding with a D_2 or a DT molecule, described by the energy-dependent rates $\lambda^0_{dt\mu-d}$, $\lambda^1_{dt\mu-d}$, $\lambda^0_{dt\mu-t}$, and $\lambda^1_{dt\mu-t}$).

Figure 12 shows the contributions of these components to the neutron time spectra. At a temperature of 30 K, molecular formation on DT molecules becomes important only at rather high tritium concentrations. The only rate that is significant for thermalized $t\mu$ atoms at this temperature is $\lambda^0_{dt\mu-d}$. Therefore, in the steady state, where the majority of $t\mu$ atoms are thermalized, molecular formation on D_2 is the most important process even at high tritium concentrations. Molecular formation by $t\mu_{F=1}$ in the steady state is important only at low tritium concentrations ($c_t < 0.10$), where spin flip is strongly suppressed, as can only occur by charge exchange on a triton (in the nonrelativistic approximation). Even in the steady state the $\lambda^1_{dt\mu-d}$ contribution is nearly exclusively due to epithermal $t\mu$ atoms because of this rate's low value for thermalized $t\mu$'s. At higher tritium concentrations the $F = 1$ state depopulates quickly and plays a role only at early times (in the region of the epithermal peak).

At high tritium concentrations $c_t \gtrsim 0.8$ the $t\mu_{F=1}$ state depopulates at a $t\mu$ energy above the region of the most prominent epithermal peak in the molecular formation rate (~ 0.3 eV). (The molecular formation peaks for DT

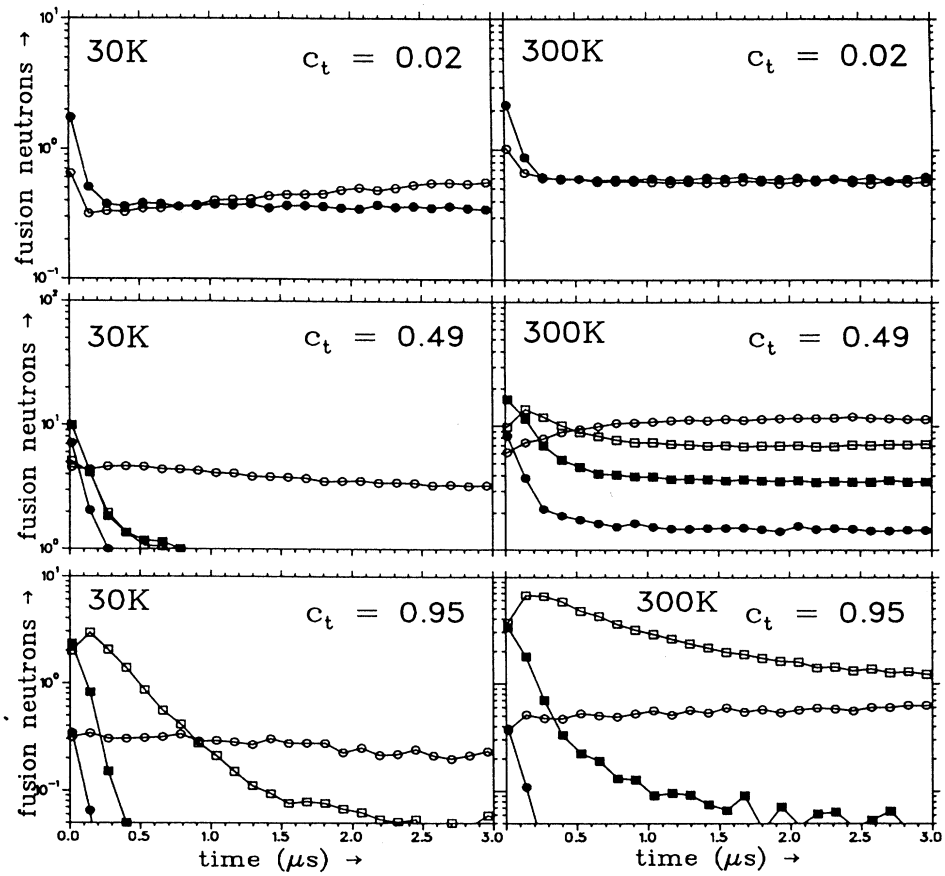

FIG. 12. Contributions of the rates $\lambda^0_{dt\mu-d}$ (open circles), $\lambda^1_{dt\mu-d}$ (filled circles), $\lambda^0_{dt\mu-t}$ (open squares), and $\lambda^1_{dt\mu-t}$ (filled squares) to the molecular formation process.

are at a lower energy than the corresponding peaks for D_2.) After this, thermalization proceeds with the low elastic scattering rate for $t\mu_{F=0} + t$. Consequently, for high c_t the fusion neutron peak at early times consists of two parts, one with a higher disappearance rate due to $t\mu_{F=1}$ depopulation and the other with a lower disappearance rate due to $t\mu_{F=0}$ thermalization. In order to find out which rates are responsible for the disagreement between theory and experiment, it is also important to differentiate between molecular formation by thermalized and by epithermal $t\mu$ atoms. Figure 13 shows these two contributions to the spectra of Figs. 11 and 12 for a target temperature of 30 K. It is obvious that in the steady state the importance of epithermal molecular formation falls strongly as the tritium concentration rises. This is readily explained by the fact that at high c_t a $t\mu$ atom has a chance of losing energy through collisions with tritons before meeting a deuterons with which it might form a muonic molecular ion.

Figures 12 and 13 show that at a target temperature of 30 K and at all except very low tritium concentrations ($c_t < 0.1$) the steady-state neutron production rate (cycling rate) depends mainly on the value of $\lambda^0_{dt\mu-d}$ for thermalized $t\mu$ atoms. At low c_t the cycling rate is not very sensitive to molecular formation rates at all, but depends mostly on the deuterium-tritium transfer process. In Fig. 14, for a target temperature of 30 K, $\lambda^0_{dt\mu-d}$ in the energy interval $0 \leq E_{t\mu} \leq 0.04$ eV was increased from its theoretical value of $\sim 40\ \mu s^{-1}$ [8] to a value of $130\ \mu s^{-1}$ (normalized to liquid hydrogen density; cf. Table III). The initial energy distribution of $t\mu$ atoms formed by muon capture was slightly adjusted (cf. Table IV). The resulting Monte-Carlo spectra (solid lines) are in good agreement with the experimental neutron spectra (error bars).

While at 30 K the steady-state cycling rate is dominated by the $t\mu_{F=0} + D_2$ component, at a target temperature of 300 K all components play an important role. Due to the target molecules' thermal motion the epithermal resonances in all relevant molecular formation rates ($\lambda^0_{dt\mu-d}$, $\lambda^1_{dt\mu-d}$, $\lambda^0_{dt\mu-t}$, and $\lambda^1_{dt\mu-t}$) become so wide that they strongly overlap with the Maxwell distribution at 300 K. So it is more difficult than at 30 K to disentangle these contributions and to differentiate between epithermal and thermal molecular formation. Due to this overlap the calculated fusion yield is much higher than at 30 K, which is not supported by the experimental data. By reducing the molecular formation rates used for the calculation the agreement with experiment can be significantly improved (Fig. 14; cf. Tables III and IV). The

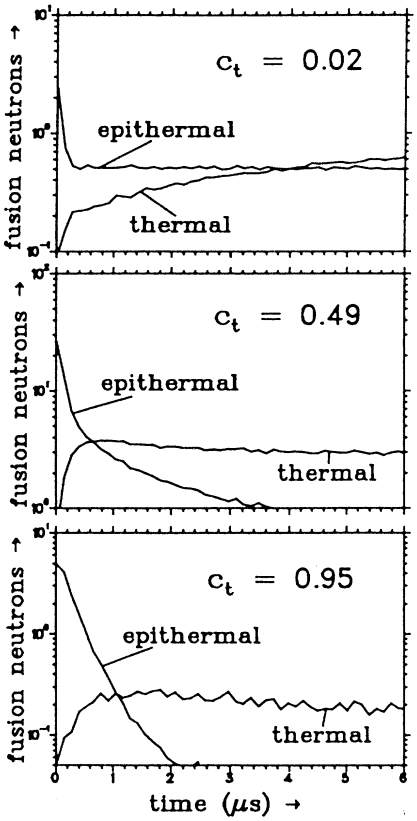

FIG. 13. Contributions of epithermal and thermal $t\mu$ atoms to the fusion neutron output.

theoretical molecular formation rates for 100 K and 200 K must also be reduced to fit the corresponding experimental data.

2. *Scattering cross sections*

The calculated fusion neutron yield does not depend on the $t\mu$ scattering very strongly. Figure 15 shows how variations in the elastic $t\mu + d$ scattering rate affect the calculated fusion neutron time distributions. The three time spectra were calculated by leaving the scattering cross section at the theoretical value [23] (central line), by increasing it by a factor of 2 (bottom line), and by reducing it by a factor of 2 (top line). The sensitivity to variations in the $t\mu + t$ cross sections at all but very high tritium concentrations ($c_t > 0.9$) is still smaller. This weak dependence of the fusion yield on the scattering cross sections in spite of the general importance of epithermal molecular formation may be understood by separately regarding the situation at various tritium concentrations.

At low c_t a large number of molecular formations in the steady state are supposed to be due to epithermal $t\mu$ atoms, but the neutron output depends rather on the production rate of $t\mu$ atoms by $d \rightarrow t$ transfer than on the subsequent molecular formation, which is comparatively fast. Although a change in the elastic $t\mu + d$ scattering rate significantly affects the ratio of molecular formations by epithermal and thermalized $t\mu$ atoms, the overall change in the neutron output is small, as may be illustrated by the following example. At $c_t = 0.02$ it does not make a big difference whether the molecular formation occurs with the thermal rate of $\sim 120\Phi\ \mu s^{-1}$ or an epithermal rate of $5000\Phi\ \mu s^{-1}$ because the corresponding times (800 ns or 20 ns, respectively) are both much smaller than the transfer time of $(\lambda_{dt} c_t \Phi)^{-1} = (270 \times 0.02 \times 0.01)^{-1} = 18.5\ \mu s$.

At intermediate tritium concentrations epithermal molecular formation seems to be responsible only for a relatively small percentage of molecular formations in the steady state. So even a significant change in the number of epithermal molecular formations results only in a small modification of the total neutron output.

At high tritium concentrations epithermal molecular formation is only of very minor importance in the steady state. Moreover, $t\mu + d$ elastic scattering is no longer dominant and the much smaller elastic cross section for $t\mu_{F=0} + t$ as well as thermalization by epithermal molecular formation and subsequent backdecay begin to play a role. This means that modifying the rate of any one of these processes influences the overall thermalization rate only weakly. The elastic process $t\mu_{F=1} + t$ is only important at $t\mu$ energies $\gtrsim 0.5$ eV, which is well above the strongest resonances in $\lambda_{dt\mu-t}$. This is due to the fact that the fast spin-flip process $t\mu_{F=1} \rightarrow t\mu_{F=0}$ becomes irreversible below this energy. So, even the size and the slope of the epithermal peak are not very sensitive to small changes in one of the scattering rates.

Considering the low sensitivity of the calculated fusion neutron spectra to the scattering cross sections and the good agreement between different calculations of these cross sections [22–24] it seems highly unlikely that modifications of the theory will strongly influence the outcome of our analysis. Even by strongly modifying the scattering cross sections it is not possible to describe the experimental data without changes in the theoretical molecular formation rates.

3. *Other parameters: The $d \rightarrow t$ transfer rate, q_{1s}, and the initial energy distribution of $t\mu$ atoms*

Deuterium-tritium transfer both in the $1s$ state of the $d\mu$ atom (with rate λ_{dt}) and in its excited states (with probability $1 - q_{1s}$) is an important process at low tritium concentrations, where most muons are first captured by a deuteron. The "transfer rate" λ_{dt} only affects the fusion neutron output of the steady state, while the value of q_{1s} is reflected both by the steady state and by the epithermal peak in the neutron time spectra.

Another parameter that strongly influences the size of the epithermal peak is the initial energy distribution of $t\mu$ atoms that were formed by direct muon capture or by transfer in excited states (after $d \rightarrow t$ muon transfer in the $1s$ state the initial energy is always far above the important molecular formation resonances). Even at low

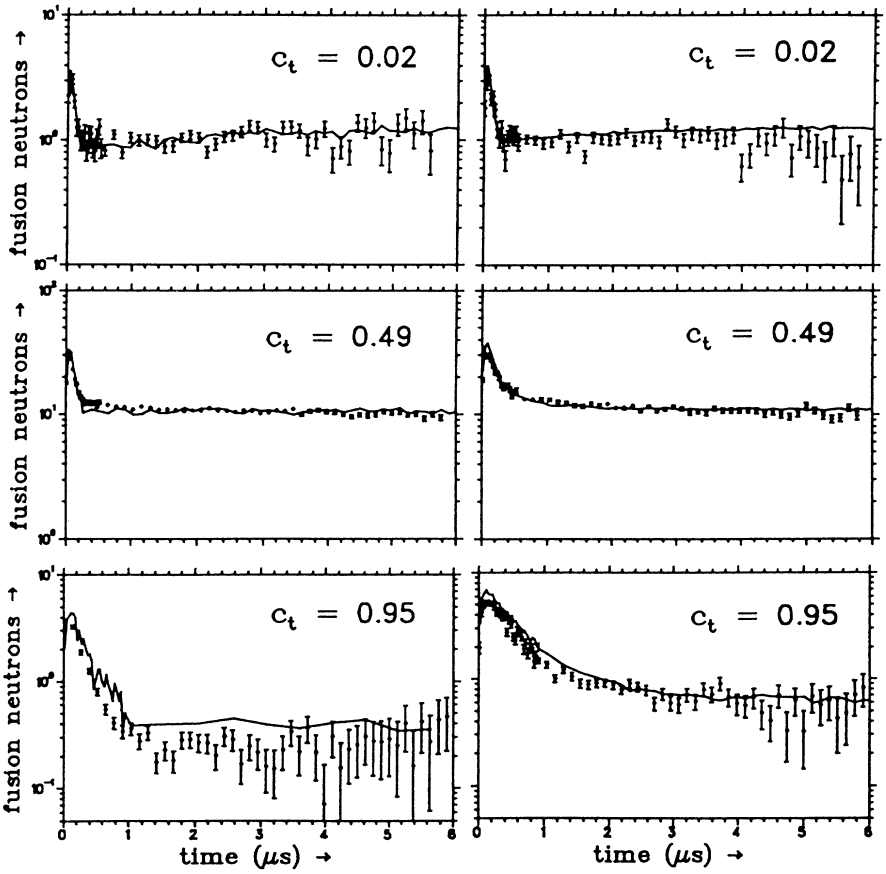

FIG. 14. Fit of experimental (error bars) fusion neutron time distributions by modifying molecular formation rates and initial $t\mu$ energy distributions (see text).

tritium concentrations, where most muons are first captured by a deuteron, the epithermal peak is due only to $t\mu$ atoms formed by direct muon capture or by $d \rightarrow t$ transfer in excited states. The fraction of $t\mu$ atoms originally thermalized after direct muon capture or excited-state transfer will be denoted by $p_{\rm th}$, while the initial energy of all other $t\mu$ atoms is supposed to lie above the important molecular formation resonances.

The value of the ground-state deuterium-tritium transfer rate λ_{dt} is supposed to be known with good accuracy [2] and the experimental spectra can be adequately described by using the theoretical values [29]. The dependence λ_{dt} on the $d\mu$ energy in a deuterium-tritium target does not strongly influence the kinetics because $d\mu$ atoms are formed with a relatively low kinetic energy of a few eV at most. The calculated fusion neutron time spectra hardly change if instead of the energy-dependent rate from [29] a constant value of $\lambda_{dt} = 270\ \mu{\rm s}^{-1}$ is used.

Some theoretical results are available for both q_{1s} [27, 35] and $p_{\rm th}$ [31], but the experimental spectra can be described by using several different sets of values for these parameters. The Monte Carlo spectra in Fig. 14 were obtained by using the q_{1s} values given in Table II and the values of $p_{\rm th}$ given in Table IV. If q_{1s} is increased and at the same time $p_{\rm th}$ reduced, the number of initially formed epithermal $t\mu$ atoms and thus the size of the epithermal peak in the fusion neutron spectra may be kept constant. By increasing q_{1s} over the value from [27] and adjusting $p_{\rm th}$ as in Table V, the fit of the experimental data at low tritium concentrations can be slightly improved, but the

TABLE III. Fit values of molecular formation rates in $\mu{\rm s}^{-1}$ for thermalized $t\mu$ atoms used for the Monte Carlo spectra in Fig. 14. (A dash — means that the theoretical values from [8] were not changed.)

Rate	30 K	300 K
$\lambda^{0,\rm th}_{dt\mu-d}$	130	100
$\lambda^{1,\rm th}_{dt\mu-d}$	—	10
$\lambda^{0,\rm th}_{dt\mu-t}$	—	20
$\lambda^{1,\rm th}_{dt\mu-t}$	—	—

TABLE IV. Fit values for the fraction of initially thermalized $t\mu$ atoms used for the Monte Carlo spectra in Fig. 14.

c_t	$p_{\rm th}$
0.02	0.50
0.10	0.50
0.49	0.50
0.88	0.58
0.95	0.61

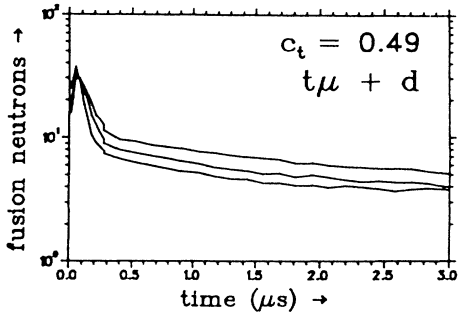

FIG. 15. Effect on the calculated fusion neutron time spectrum of increasing or decreasing the elastic scattering cross section for $t\mu + d$ by a factor of 2.

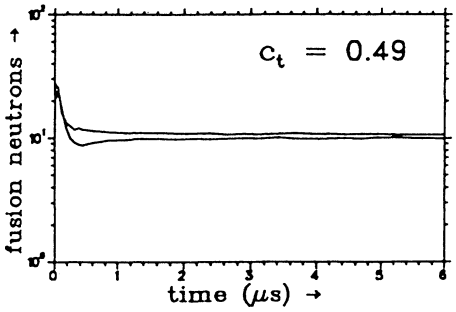

FIG. 16. Effect of increasing (top line) or reducing (bottom line) the epithermal molecular formation rate by a factor of 2 with simultaneous adjustment of the initial $t\mu$ energy distribution.

difference is not significant. Therefore the analysis of the data from the low-density deuterium-tritium experiment does not yield unequivocal information about either of these two parameters.

The third parameter that influences the epithermal peak is the epithermal molecular formation rates, i.e., the size of the molecular formation resonances at high $t\mu$ kinetic energies. Figure 16 shows that by increasing or decreasing these rates and the value of $p_{\rm th}$ at the same time, very similar time spectra may be produced. This makes it difficult to draw conclusions concerning the absolute size of the epithermal molecular formation resonances from deuterium-tritium data alone. However, important complementary information may be obtained from our H-D-T triple mixture experiment.

D. Analysis of data from the H-D-T experiment

Due to the Ramsauer-Townsend effect in the scattering of $d\mu$ and $t\mu$ on ^{1}H, the protons become practically "invisible" for muonic atoms in the energy region close to and above the major molecular formation resonances. At high ^{1}H concentration most deuterons are bound in HD molecules and the main contribution to muon-catalyzed dt fusion comes from $[(dt\mu)pee]$ molecular complexes formed with rate $\lambda_{dt\mu-p}$. The tritium concentration was so low that direct muon capture by tritons can be neglected and the initial $t\mu$ population is mostly due to the fast $p \rightarrow t$ transfer in the muonic atoms' ground state, which guarantees that the $t\mu$ atoms are formed with a very high initial energy (46 eV) far above the molecular formation resonances. This excludes the uncertainties due to the unknown initial $t\mu$ energy distribution in the D-T experiment.

Unlike a deuterium-tritium target, due to the low deuterium concentration ($0.03 \leq c_d \leq 0.1$), most $d\mu$ atoms are formed by $p \rightarrow d$ transfer with high initial energy of $\sim$ 45 eV. As the theoretical rate [29] for $d \rightarrow t$ transfer at such an energy is larger, by nearly two orders of magnitude, than at thermal energies, it competes successfully with $d\mu$ thermalization and Monte Carlo calculations show that a significant part of the initial peak in fusion neutron time spectra in H-D-T mixtures is due to this epithermal $d \rightarrow t$ transfer. The initial kinetic energy of $t\mu$ atoms formed by this transfer process ($\sim$ 19 eV) is also well above the molecular formation resonances. In deuterium-tritium targets that do not contain any ^{1}H the initial $d\mu$ energy of a few eV at the most is not sufficient for epithermal $d \rightarrow t$ transfer to play an important role.

A comparison of the experimental data from the H-D-T experiment and their Monte Carlo simulation with the molecular formation rates from [8] shows that the size of the epithermal peak is significantly overestimated by the theory (see Fig. 17). Due to the low deuterium and tritium concentrations most epithermal $dt\mu$ molecular formations occur during collisions of $t\mu$ atoms with HD molecules. So the H-D-T experiment yields a measurement of the molecular formation rate $\lambda_{dt\mu-p}$.

TABLE V. Alternative set of values for q_{1s} and $p_{\rm th}$.

c_t	$p_{\rm th}$	q_{1s}
0.02	0.00	1.00
0.10	0.25	0.97

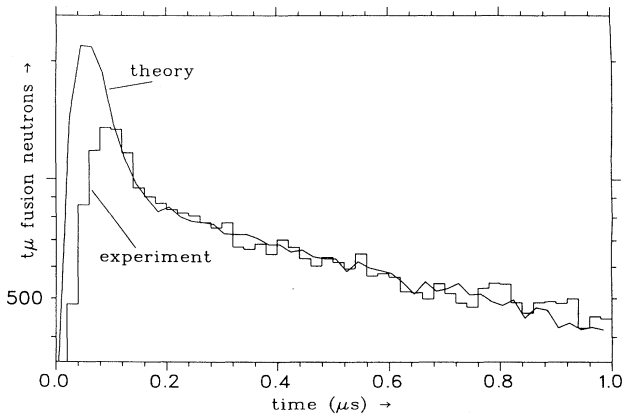

FIG. 17. Experimental (histogram) and calculated fusion neutron time spectra in a H-D-T triple mixture (target parameters: $c_p = 0.97$, $c_d = 0.03$, $c_t = 36\times10^{-5}$, and $\Phi = 17\%$).

However, there should be no qualitative difference between molecular formations by $t\mu$ atoms interacting with HD, DT, or D_2 molecules and it may be expected that conclusions may be drawn from this result also for $\lambda_{dt\mu-d}$ and $\lambda_{dt\mu-t}$.

IV. RESULTS AND DISCUSSION

A. Molecular formation rates

Monte Carlo calculations have shown that molecular formation by epithermal $t\mu$ atoms is important not only at early times and low target densities, where their contribution appears as a visible peak in the time spectra of fusion neutrons, but also in the steady state and at high densities. In a deuterium-tritium target the fraction of molecular formations in the steady state due to epithermal $t\mu$ atoms rises from less than 10% at high tritium concentrations ($c_t > 0.9$) to nearly 40% at low tritium concentrations ($c_t < 0.1$). The neutron time distributions depend mostly on the integral of the molecular formation resonances over the energy distribution of muonic tritium atoms. So the absolute size of these resonances can be checked by fitting the time spectra, but it is not possible to draw accurate conclusions concerning their exact position and shape.

While the theoretical molecular formation rates yield a good qualitative description of the experimental data, there remain significant quantitative discrepancies.

(i) The rate for $dt\mu$ formation by thermal muonic tritium atoms in the $F = 0$ hyperfine state at a target temperature of 30 K and a target density of $\phi = 1\%$ obtained by fitting the experimental data is $\lambda_{dt\mu-d}^{0,\mathrm{therm}} = 130 \pm 20\ \mu\mathrm{s}^{-1}$ and is thus significantly higher than the value of $\sim 40\ \mu\mathrm{s}^{-1}$ predicted by theory [8].

(ii) The $dt\mu$ formation rates at target temperatures of 100–300 K are overestimated by theory [8]. The theoretical rates would result in a strong temperature dependence of the fusion neutron yield between 30 K and 300 K at all tritium concentrations, while the experimental spectra show practically no dependence at low tritium concentrations ($c_t \lesssim 0.1$) and a much smaller one at higher tritium concentrations. The fit values for the rates of molecular formation by thermal $t\mu$ atoms at 300 K in a deuterium-tritium target given in Table III may serve as a guideline. Because of the unknown initial energy distribution of $t\mu$ atoms, the size of the epithermal resonances of $\lambda_{dt\mu-d}$ and $\lambda_{dt\mu-t}$ could not be determined directly, but complementary data from an experiment in a triple H-D-T mixture suggest that the epithermal resonances of the analogous $\lambda_{dt\mu-p}$ rate have been significantly overestimated in [8].

B. Other parameters of the kinetics model

The Monte Carlo analysis of the thermalization of muonic atoms has shown that the time distributions of fusion neutrons are not very sensitive to minor modifications of elastic scattering and spin-flip cross sections. The angular anisotropy of some cross sections (in particular for $t\mu + d$ scattering) strongly influences the thermalization process, while atomic and molecular effects (including electron screening) are not very important in this context. The experimental data are adequately described by the theoretical cross sections [23, 25], which are in agreement with other calculations [22, 24].

The deuterium-tritium ground-state transfer rate λ_{dt} as calculated in [29] is in agreement with the experimental data. The energy dependence of λ_{dt} ("epithermal dt transfer") becomes important at conditions where $d\mu$ atoms are formed by $p \rightarrow d$ transfer with very high initial kinetic energy. Deuterium-tritium transfer in excited states as described by the q_{1s} parameter may be significant, but is hard to analyze without sufficient information about the initial energy distribution of $t\mu$ atoms. Our experimental data favor somewhat higher values of q_{1s} (i.e., less transfer in excited states) than predicted by theory [27], but the evidence cannot be regarded as conclusive.

The initial energy distribution of $t\mu$ atoms not formed by ground-state transfer was approximated by using a phenomenological parameter p_{th}. This parameter describes the fraction of initially thermalized muonic tritium atoms while the rest is considered to have an energy higher than the main molecular formation resonances. The data suggest that p_{th} rises with the tritium concentration, but in order to extract absolute values, assumptions have to be made for the rates of epithermal molecular formation and, at low tritium concentrations, for the q_{1s} parameter. If the epithermal molecular formation rates [8] are used, p_{th} ranges from 0.5 to 0.7 for $c_t \geq 0.5$. If they were smaller by a factor of 2, as suggested by our H-D-T experiment as well as by recent calculations [34], p_{th} would range from 0.3 to 0.5 for the same range of tritium concentrations. For lower tritium concentrations p_{th} between 0.5 and zero is obtained, depending on the assumed values of q_{1s} and epithermal molecular formation.

V. CONCLUSIONS AND OUTLOOK

An overall understanding of epithermal phenomena in muon-catalyzed deuterium-tritium fusion has been achieved. Experimental data and theoretical calculations are in agreement with regard to the importance of epithermal molecular formation for $dt\mu$ kinetics. Still, the picture has yet to be refined in certain respects. The most important remaining discrepancies between theory and experiment are the following.

(i) In general, the molecular formation rates seem to be somewhat overestimated by the theory [8].

(ii) The rate $\lambda_{dt\mu-d}^{0,\mathrm{therm}}$ for molecular formation by thermalized $t\mu$ atoms in the $F = 1$ hyperfine state colliding with D_2 molecules in a cryogenic target (~30 K) is underestimated in these calculations.

It has been suggested [36] that the dipole approximation used in calculations [8] may give rise to significant errors. This might explain the first discrepancy. The second problem could be due to the influence of subthreshold resonances in the molecular formation rates, which due to the natural linewidth might influence the region above

the energy threshold. Both factors have been taken into consideration by recent calculations [34], which seem to show better, although not perfect, agreement with experiment than [8]. These calculations have not yet been finished and an overall comparison with experimental data is still not possible. Another reason contributing to the second discrepancy might be that $\lambda_{dt\mu-d}^{0,\mathrm{therm}}$ differs significantly for ortho- and para-D_2 and the ratio of these two populations is not well known because ortho-para transitions might be catalyzed by the β decay of the tritium in the target.

An ambitious experiment to measure molecular formation in the region of the "epithermal" resonances by heating up a target to a temperature of 2000 K and thus making these resonances accessible for thermalized muonic tritium atoms is being planned at PSI [10]. The experimental difficulties of handling tritium at such high temperatures and the resulting high pressures are enormous, but the results will be invaluable as they will demonstrate the supposed maximum fusion yield independent of any kinetical parameters.

While scattering cross sections for muonic atoms and ground-state muon transfer rates seem to be sufficiently well known for analyzing epithermal effects, our knowledge of cascade processes and muon transfer in excited states (described by q_{1s}) as well as of the initial energy distribution of muonic atoms after muon capture is far from satisfactory. Experiments that directly measure q_{1s} for the H-D case have been carried out [28, 37] and are currently being evaluated. An extension of these measurements to the D-T case may be envisaged at a later date.

ACKNOWLEDGMENTS

We would like to thank all our colleagues who worked with us during the experiments and their analysis, in particular our colleagues at IMEP, SPNPI, PSI, TU Munich, and LBL. It is a pleasure to thank A. Adamczak, V.E. Markushin, V.S. Melezhik, Yu.V. Petrov, V.Yu. Petrov, and L.I. Ponomarev for many fruitful discussions on the theory of muon-catalyzed fusion. Financial support by the Austrian Science Foundation, the German Federal Ministry of Research and Technology, Paul Scherrer Institute, the Swiss National Foundation, and the U.S. Department of Energy is gratefully acknowledged.

[1] F.C. Frank, Nature **160** 525 (1947); Ya.B. Zel'dovich and S.S. Gerstein, Usp. Fiz. Nauk **71**, 581 (1960) [Sov. Phys. Usp. **3**, 593 (1961)].
[2] W.H. Breunlich, P. Kammel, J. Cohen, and M. Leon, Annu. Rev. Nucl. Part. Sci. **39**, 311 (1989).
[3] W.H. Breunlich *et al.*, Phys. Rev. Lett. **53**, 1137 (1984).
[4] W.H. Breunlich *et al.*, Muon Catalyzed Fusion **1**, 67 (1987).
[5] P. Kammel, Nuovo Cimento Lett. **43**, 349 (1985).
[6] J. Cohen and M. Leon, Phys. Rev. Lett. **55**, 52 (1985).
[7] S. Jones *et al.*, Phys. Rev. Lett. **51**, 1757 (1983).
[8] M.P. Faifman *et al.*, Muon Catalyzed Fusion **4**, 1 (1989); **4**, 341 (1989); M.P. Faifman and L.I. Ponomarev, Phys. Lett. B **265**, 201 (1991).
[9] W.H. Breunlich, Nucl. Phys. A **478**, 769c (1988).
[10] J. Zmeskal *et al.*, Muon Catalyzed Fusion **5/6**, 379 (1990).
[11] G. Marshall, in *Muonic Atoms and Molecules*, edited by L.A. Schaller and C. Petitjean (Birkhäuser, Basel, 1993), p. 251.
[12] K. Lou, in *Muonic Atoms and Molecules* (Ref. 11), p. 147; V.E. Markushin, *ibid.*, p. 267.
[13] R. Sherman and J. Zmeskal (unpublished).
[14] J. Marton *et al.* (unpublished).
[15] M. Cargnelli, Ph.D. thesis, Technical University of Vienna, 1987.
[16] N. Nägele *et al.*, Nucl. Phys. A **493**, 397 (1989).
[17] J. Zmeskal *et al.*, Phys. Rev. A **42**, 1165 (1990).
[18] W.H. Breunlich *et al.*, Phys. Rev. Lett. **58**, 329 (1987).
[19] P. Ackerbauer, Ph.D. thesis, University of Vienna, 1992.
[20] S.E. Jones *et al.*, Phys. Rev. Lett. **56**, 588 (1986).
[21] J. Werner, Ph.D. thesis, University of Vienna, 1990.
[22] M. Bubak and M.P. Faifman, JINR Communication No. E4-87-464, Dubna, 1987 (unpublished).
[23] L. Bracci *et al.*, Muon Catalyzed Fusion **4**, 247 (1989); C. Chiccoli *et al.*, *ibid.* **7**, 87 (1992).
[24] J. Cohen, Phys. Rev. A **43**, 3460 (1991); **43**, 4668 (1991); **44**, 2836 (1991).
[25] A. Adamczak and V.S. Melezhik, Muon Catalyzed Fusion **4**, 303 (1989); A. Adamczak *et al.*, *ibid.* **7**, 309 (1992).
[26] A. Adamczak, Hyperfine Interact. **82**, 91 (1993).
[27] L.I. Menshikov and L.I. Ponomarev, Pis'ma Zh. Eksp. Teor. Fiz. **39**, 542 (1984) [JETP Lett. **39**, 663 (1984)].
[28] P. Ackerbauer *et al.*, Paul Scherrer Institute Newsletter 1991, p. 53 (unpublished).
[29] A. Adamczak *et al.*, Phys. Lett. B **285**, 319 (1992).
[30] L. Bracci and G. Fiorentini, Nuovo Cimento A **43**, 9 (1978).
[31] L.I. Menshikov, Muon Catalyzed Fusion **2**, 173 (1988).
[32] R. Siegel, in *Muonic Atoms and Molecules* (Ref. 11), p. 243.
[33] M. Jeitler, Ph.D. thesis, University of Vienna, 1992.
[34] Yu.V. Petrov and V.Yu. Petrov, Zh. Eksp. Teor. Fiz. **100**, 56 (1991) [Sov. Phys. JETP **73**, 29 (1991)]; Yu.V. Petrov, Pis'ma Zh. Eksp. Teor. Fiz. **55**, 556 (1992) [JETP Lett. **55**, 577 (1992)]; Yu.V. Petrov and H. Schmidt (private communication).
[35] W. Czaplinski *et al.*, Los Alamos National Laboratory Report No. LA-12698-C, p. 314, 1994 (unpublished).
[36] A. Scrinzi, Muon Catalyzed Fusion **5/6**, 179 (1990).
[37] B. Lauss *et al.*, Los Alamos National Laboratory Report No. LA-12698-C, p. 300, 1994 (unpublished).